Oncology

Oncology and Informatics – Research Article

Oncology 2024;102:515–524
DOI: 10.1159/000533773

Received: April 18, 2023
Accepted: August 17, 2023
Published online: November 25, 2023

Co-Culture Device for in vitro High Throughput Analysis of Cancer-Associated Fibroblast and Cancer Cell Interactions

Adam Germain[a] Young-Tae Kim[a, b]

[a]Department of Bioengineering, University of Texas at Arlington, Arlington, TX, USA; [b]Department of Urology, University of Texas Southwestern Medical Center, Dallas, TX, USA

Keywords
H460 · Cancer-associated fibroblasts · Co-culture · High throughput

Abstract
Introduction: Cancers in general, and specifically lung cancer, continue to have low patient survival rates when the patient is at an advanced stage when diagnosed. It appears that the local environment, especially fibroblasts and their signaling molecules, tends to induce metastasis, increase cancer cell resistance to treatment, and aid in tumor growth rates. Since 3-D models quickly become too complex and/or expensive and therefore rarely leave the lab they are developed in, it is interesting to develop a 2-D model that more closely mimics clustered tumor formation and bulk interaction with a surrounding fibroblast environment. ***Methods:*** In the present study, we utilize an off-the-shelf stereolithography 3-D printer, standard use well plates, magnets, and metallic tubes to create a customizable 2-D co-culture system capable of being analyzed quantitatively with staining and qualitatively with standard fluorescent/brightfield microscopy to determine cancer-fibroblast interactions while also being able to test chemotherapeutic drugs in a high-throughput manner with standard 96-well plates. ***Results:*** Comparisons from monoculture and co-culture growth rates show that the presence of fibroblasts allows for significantly increased growth rates for H460 cancer. Additionally, the viability of cancer cells can be quantified with simple cell staining methods, and morphology and cell-cell interactions can be observed and studied. ***Discussion:*** The high throughput model demonstrates that boundary condition changes can be observed between cancer cells and fibroblasts based upon the different chemotherapeutics that have been administered.

Introduction

Lung cancer is the third most common cancer in occurrence behind skin cancer and breast cancer for women and prostate cancer for men in the USA but consists of 18% of all cancer deaths worldwide, making it the deadliest cancer [1–3]. While the progress in early detection and treatment combined with reduced rates of smoking are certainly helping, lung cancer will continue as the deadliest cancer for two factors – "vaping" is creating a resurgence in smoking tobacco and other chemicals, especially in younger generations, and many people who develop lung cancer discover the cancer later in their lifespan and only find out when the cancer is already in stage III or IV of progression which is further along than most current treatments can handle [1, 2]. Early detection for lung cancer is a promising target for research, but the fact is that it is difficult to screen entire

karger@karger.com
www.karger.com/ocl

Correspondence to:
Young-Tae Kim, ykim@uta.edu

Karger

populations of people at or above 55 or even 65 years of age for a single type of cancer, so there needs to be further research into combating more aggressive versions of cancers to improve 5-year survival rates above their currently dismal percentages [2, 3].

The objective of in-vitro cancer experimentation is to find a solution that both matches important aspects of the natural environment of the cancer and is relatively quick and simple to test so that meaningful results can be acquired as quickly as possible. One of the most important environmental characteristics to mimic is the combination of healthy fibroblasts and cancerous cells and the effects of their communication. It is well established that tumor cells actively communicate with fibroblasts in their environment, and the interactions between the two cell types cause greater cell growth and enhanced metastasis capabilities for the tumor cells [4–6]. There are studies that measured upregulation of matrix metalloproteinase 1 (MMP-1), vascular endothelial growth factor (VEGF), glucose transporter 1 (GLUT1), and others in different co-culture models, demonstrating that the interactions between cancer and fibroblasts are based on some commonly overexpressed factors in malignant tumors [6–8]. These malignant tumors are the deadliest, causing 86% of lung cancer patients diagnosed with distantly spread cancer to only have a 5% survival rate for 5 years [1, 3]. The desire for rapid testing in a co-culture setting is to understand which drugs impact malignant tumors effectively and which drugs allow the healthy fibroblasts to survive and regrow. While there are many different proteins and pathways that need to be studied to elucidate interactions in greater detail, there is also a need to study effects of different therapeutics for these cancer models in parallel so that gains, even small ones, can be made for patient survival.

There are currently many different types of drug testing models available in both 2D and 3D. Models involving 2D testing tend to rely on mixed co-cultures or growth of one subtype followed by addition of a second after some days [9–11]. These methods show more of a scattered tumor model where single cells or small clusters are spread throughout the healthy fibroblast cell environment. While they do involve direct co-culture methods, standard tumors tend to grow from individual cells into large masses where they can accelerate their own malignancy with physical crowding causing excretion of specific proteins and the induction of epithelial to mesenchymal transition (EMT) [12, 13]. Some researchers search for paracrine signaling by separating the cell types in culture such as Boyden assays with trans-well inserts [14–18] or custom microfluid devices, allowing only media sharing with cyclic flow of media or manual switching of conditioned media [19, 20]. These studies are helpful for understanding distance communication between fibroblasts and cancer cells, and their results are simpler to quantify, but they lack any juxtacrine signaling taking place. Additionally, there have been attempts at creating more reliable scratch assay wound healing models that involve creating distinct spaces with polydimethylsiloxane (PDMS) inserts, but these studies have found that PDMS leaves a residue on the surface of the well plates that significantly retards cell migration into the void after removal [21, 22]. Models involving 3D testing can suffer from several different types of problems due mostly to the increasing complexity inherent in adding another dimension to the analysis. Some studies create 3D devices out of Matrigel or other novel scaffolds [23–25] or utilize hanging-drop methods [12, 26] of culture to generate spherical co-cultures. These devices require preparation of different scaffold materials and require increased processing, involving flow cytometry or fixing the cells and observing them outside of their live environment because 3D cultures can be difficult to image. There are magnetic microfluidic devices utilizing magnets both below and above the well plates and aim to create specific 2D patterns or 3D spherical cultures based upon prior incubation of cells with proprietary magnetic nanoparticles [26–28]. The magnetic devices are like those used in the proposed method but require proprietary nanoparticles and difficult media changes to create and preserve the 3D spherical structures that are grown [27, 28]. While these studies are valuable to understanding different functions and features of cancer and healthy cell interactions in environments that are approaching in vivo conditions, the current 2D and 3D methods are lacking a high throughput method of quickly and simply understanding therapeutic interactions with both cancer and healthy cells simultaneously.

In the current study, we investigated the interactions between primary cell line human dermal fibroblast-α cells (HDF-α) and epithelial lung cancer line cells (H460) in a 2D cell culture model involving simultaneous seeding of the cultures on a well plate holder embedded with magnets to create an island of H460 among the HDF-α via a metal tube so that we could determine the effects that migration, invasion, and cancer associated fibroblast (CAF) cell signaling would have upon various common therapeutic treatments. The importance of the well-plate holder and tube is that they enable an open space between the cell types during seeding but leave no residue behind that might prevent the cells from crossing the boundary after the tube has been removed, and they utilize any type

of standard well plate, so the system can be integrated into any machine that uses current well plate designs. This allows for drug studies to be initiated as early as 24 h after initial seeding as the two cultures will have already made physical contact with each other.

Materials and Methods

Cell Lines and Culture and Reagents

The human dermal fibroblast α (HDF-α) and human NSCLC line NCI-H460 were purchased from ATCC and cultured in RPMI media supplemented with 10% of fetal bovine serum with both cell lines grown in 37°C and 5% CO_2. The therapeutics Paclitaxel (Taxol, PHL89806), Doxorubicin (Dox, D1515), 5-Fluorouracil (5-FU, 343922), Chlorotoxin (CTX, C5238), Calcitriol (1086312), and Blebbistatin (203391) were purchased from Sigma-Aldrich. Anycubic Photon Mono and Anycubic 3D Printer 405 nm SLA UV-Curing Resin were purchased from Amazon. PDMS and curing agent were purchased from ThermoFisher Scientific. CellTracker™ Orange CMTMR Dye (C2927) and Hoechst 33342 (H3570) were purchased from ThermoFisher Scientific. Green Live/Dead Stain (6342) was purchased from Immunochemistry Technologies.

Device Design and Fabrication

Lung tumor microenvironment involves a complex set of cells including endothelial cells, healthy epithelial cells, fibroblast cells, and immune cells and the devices were created with this in mind. The co-culture devices were fabricated by utilizing stereolithography (SLA) resin 3D printing techniques, and poly (dimethyl siloxane) (PDMS) inserts for cell culture medium boundary were made with molding techniques.

A magnet embedded well plate holder was created in Solidworks design software utilizing the dimensions given online for standard 96-well, 12-well, and 6-well plates to fit any well plate and line-up the magnets with the center point of each well. A mock-up of the well plate was utilized to determine if the dimensions of the holder would fit properly and if the magnets would be centered beneath each well. The magnet dimensions were measured, and slightly larger holes were created in the holder to ensure a secure fit for each magnet. An AnyCubic Photon Mono resin 3D printer was utilized to create the modeled plate holder. They were set-up on a side and printed with a layer thickness of 0.05 mm, 6 bottom layers with exposure of 45 s, normal exposure time of 2 s, Z lift of 6 mm, and Z lift speed of 4 mm/s. No additional supports were required to generate a functional product.

The PDMS inserts were created by first mixing a 10:1 ratio of polymer to curing agent, and then degassing under 500 mm Hg vacuum in a chamber for 30 min. After degassing, a silicon wafer was pre-heated on a hotplate to 75°C and the PDMS mixture was poured onto the wafer until approximately 5 mm thick, then left for 2 min to allow any bubbles formed from pouring to be removed from the polymer. The silicon wafer was then transferred to a 150°C hotplate for 5 min. Upon solidification, the wafer and PDMS were removed from the hotplate and allowed to cool for 2–5 min and the PDMS was cut out and peeled off the wafer in a single circular piece and allowed to cool and finish curing overnight. The following day, the PDMS was cut into roughly square pieces, smaller than the well sizes for the 6-well and 12-well plates, and each piece was punched in the center with an 8-mm-diameter hole punch tool. The PDMS inserts had any larger contaminating material removed by tape and were immersed in 70% ethanol in an enclosed container for 30 min for sterilization. These were then taken into a hood, washed three times in sterile deionized water, and allowed to dry inside the hood overnight before being placed into the well plates.

The co-culture device assembly requires the resin well plate-holder, the magnets to be inserted into the plate-holder, the PDMS inserts, and the metal tubes used to separate the different cell cultures for seeding. The PDMS inserts are not necessary for 96-well plates due to the small individual size of the wells. The magnets are first placed into the magnet holder, and the appropriate well plate is then placed on top of the holder. The PDMS inserts are then attached to the well plate such that the center of the hole punch aligns with the center of the magnet beneath the well followed by dropping the metal tubes onto the magnets. The PDMS inserts hold the cell culture medium and surrounding fibroblasts close to the metal tube where the cancer cells are seeded.

Cell Area Measurements for Growth Comparisons

Due to a lack of tracking dye retention, the HDF-α/H460 boundary area was utilized to estimate progressive growth over a 7-day-long co-culture experiment. For this experiment, 12-well plates were prepared with sterilized PDMS boundary inserts, placed onto a magnet-holder plate, and one tube was set in the center of each well inside a biosafety cabinet. The cancer cells were stained with Texas Red cell tracker prior to seeding and were seeded at a rate of 5,000 cells/well inside the tube of each well plate. HDF-α cells were seeded at 20,000 cells/well on the outside of the wall of the tube and inside the PDMS structure. After allowing the cells to attach for 3 h, the tubes and PDMS boundaries were carefully removed, and the 12-well plates were removed from the magnet holder devices. Day 0 pictures were taken at 2.5× magnification to verify that the boundary seeding was successful, and then 1 mL of RPMI growth media was added to each well. The cells were tracked for 7 days with pictures taken once per day at both 2.5× and 10× magnification. For the first 3 days, the fluorescent area could be tracked and measured for the cancer area, but after this, the fluorescent signal began to weaken. A distinct circular boundary formed between the H460 and HDF-α was utilized to measure the area of the main "tumor" progression in ImageJ software after combining the brightfield and fluorescent images.

H460 and HDF-α Co-Culture Drug Study

A 96-well magnet holder was prepared with magnets and sterilized, and a 96-well plate was placed on top of the holder while inside a biosafety cabinet. The tubes were sterilized and placed on top of the magnets, inside the selected wells for the experiment. Using an $n = 4$, the wells were seeded with 5,000 H460 cancer cells in 3 μL on the inside of the tube and 20,000 HDF-α healthy fibroblast cells in 40 μL outside of the tube. The cells were incubated for 3 hours at 37°C and 5% CO_2 to allow for attachment to the well plate. The tubes were then carefully removed in the biosafety cabinet, and then brightfield and fluorescent pictures were taken to verify the correct seeding had occurred. Then the tubes were removed and 200 μL of fresh RPMI + 10% FBS growth media was added to each well, and they were incubated for 24 h. The following day, brightfield and fluorescent images were taken of the cells and

upon confirmation of the boundary formation, the media was refreshed with 200 μL of fresh media + DMSO for control and 200 μL of media plus DMSO plus one of the following drugs for each other condition: 50 nM of paclitaxel (Taxol), 5 μM of doxorubicin (Dox), 25 μM of 5-fluorouracil (5-FU), 300 nM of chlorotoxin (CTX), 5 μM of calcitriol, or 1 μM of blebbistatin. The cells were then incubated for 2 more days and with pictures taken every 24 h of each well. Images were merged and adjusted for clarity in ImageJ software after being taken. Repeats of the experiment were done in a 48-well plate with 500 μL of fresh media/well, but were limited to the DMSO control, 50 nM of paclitaxel (Taxol), 5 μM of doxorubicin (Dox), 25 μM of 5-fluorouracil (5-FU), 300 nM of chlorotoxin (CTX) conditions. The $n = 4$, CMTMR staining of H460 cancer cells prior to seeding, seeding values of H460 at 5,000 cells/well in 3 μL and HDF-α at 20,000 cells/well in 40 μL, the duration of attachment, waiting 24 h before adding drug conditions, and 48 h incubation for imaging were maintained for the experiment. For cell counting after 48 h, all conditions were stained with 100 μL of image media containing Hoechst at 1:1,000 concentration (all cell stain) and Green Live/Dead Stain at 1:1,000 concentration (dead cell stain) for 20 min. Then images were taken at 10× magnification at the center seeding location for all wells to cover the entire main "tumor" mass. Cells fluorescing blue, red, and green were counted as "dead" cancer cells and those with red and blue fluorescence were counted as total cancer cells via ImageJ particle analyzer with a low threshold to remove non-cell particles. Live cells were calculated and then averaged for each condition.

Statistics

Statistical software R was used to generate statistical analysis. ANOVA and Tukey post hoc test was utilized to denote significant differences among multiple groups and a p value of <0.05 was considered statistically significant.

Results

Development of Low-Cost, Simple Co-Culture Device

To solve the problems found in previous studies, making a device that could aid in the study of metastasis phenotype cancer, main tumor cancer cells, and healthy cells in one place appeared to be the solution. Since it is well studied that cancer-associated fibroblasts (CAFs) can induce a metastasis-like phenotype on tumor cells, the idea came about to create an island of cancer surrounded by fibroblasts for a direct contact method of co-culturing and to help simplify the quantification of both cell types. The device shown in Figure 1 below is 3D printed from a standard, low-cost resin SLA printer that holds magnets in the indentations and can be easily customized for different sizes of magnets. The plate is designed so that standard well plates (from 6-well to 96-well) can be stably placed on top and the magnets will align with the center of each well plate. The location of the magnet allows magnetic, metallic tubes to be placed inside the wells such that they separate the plate into two distinct areas, the center of tube where the cancer cells are seeded and out of tube where fibroblasts (or other cells) are seeded. If needed for larger well plates, an additional PDMS or other device can be placed as an outer boundary to maintain a smaller distance between the healthy and cancer cells. The steps for use are as follows and can also be seen in Figure 1: first the magnet holder should be filled with magnets and then the well-plate should be placed on top. Then the desired outer boundary should be placed surrounding the magnet but inside the well plate. The tubes should be placed on top of the magnet with hole facing upwards. The cancer cells should be seeded inside the tube making sure to utilize an appropriate amount of carrying fluid, depending on the chosen tube size. The healthy cells should be seeded on the outside of the tube and then incubated for a few hours to give the cells time to attach. The tubes and any outer layer insert were removed carefully and then the normal growth media was added for the cells. The cells used in the study can be transfected cells for ease of tracking, they can be differentially stained prior to seeding, or the cells can be fixed after the study and immunostained depending on the researcher's needs. From Figure 1e, you can see the distribution of cells, red for H460 and green for HDF-α, 3 h after seeding and after removal of the tube and magnet holder. There are some cells that will move across the boundary, but the general boundary between the different cell types is kept distinct. The simplicity of the procedure, and approximate cost of ~USD 200 for the materials to make one's own plates (including the purchase of a 3D printer) make this approach quite attractive.

Co-Culture Accelerated Growth Model

The first thing to note about Figure 2 is the full 360 cellular boundary formed between the H460 and HDF-α within 24 h of seeding. The quick crossing of the open space between the two cell types shows that neither the magnetic approach nor the tube used for separation hinder cell motility. The growth of the H460 "tumor" mass was measured over 7 total days, taking advantage of the distinct ring formed by the H460 cells at the contact point with the HDF-α, and demonstrated that the with this model, the main mass of cancer quickly radiates outward with some satellite colonies forming clusters farther from the center mass. Figure 2b shows the beginning stages of an S-curve growth pattern, expected for unchecked cancer growth in favorable conditions. The area measurement method is useful for obtaining a general impression of the cancer's survivability in various conditions, comparable to the measurements of tumor mass in subcutaneous studies with immunocompromised

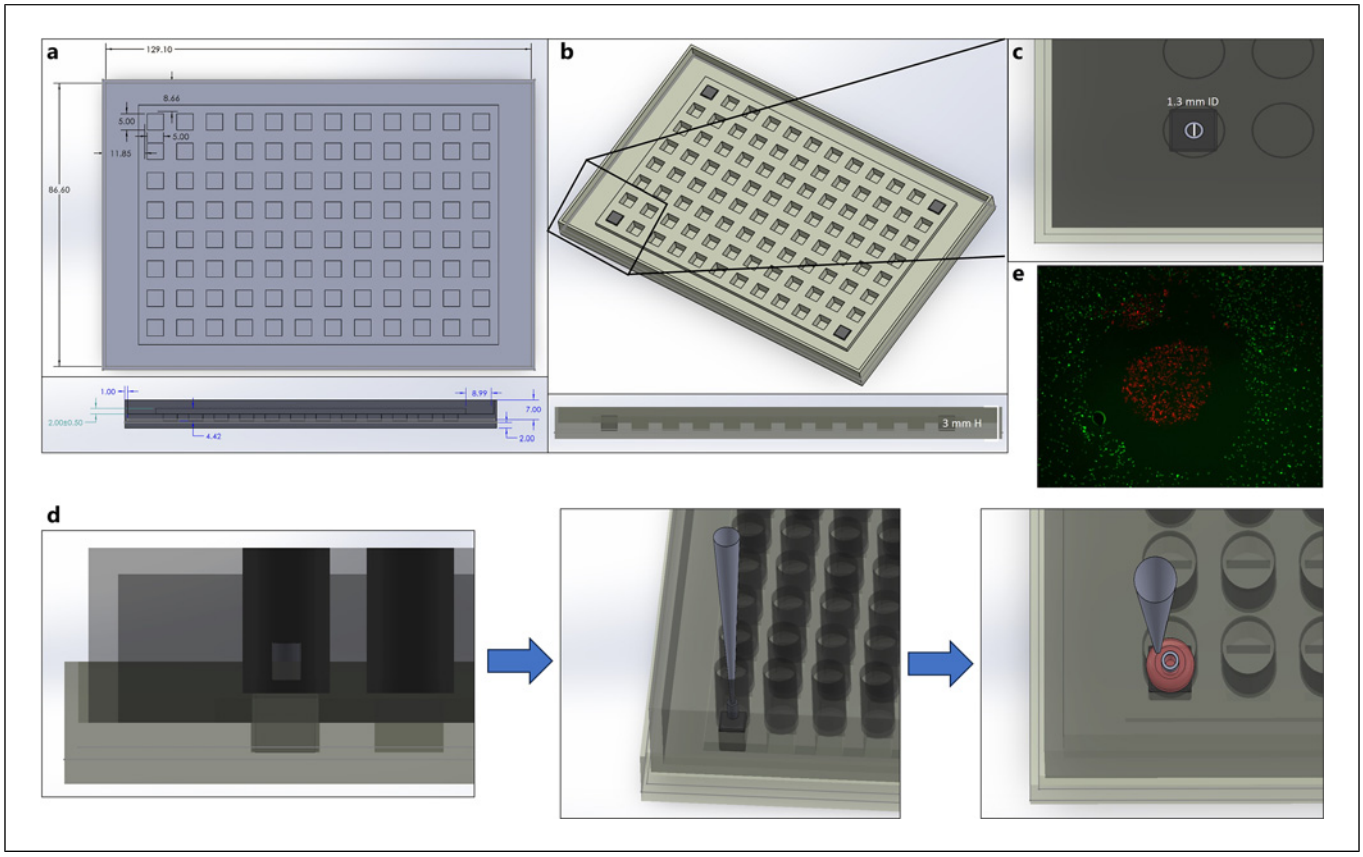

Fig. 1. Design and Implementation of the 96-well plate holder magnetic co-culture device. **a** Design and dimensions of well plate holder top and side view, measurements in millimeters. **b** Well plate holder with 4 small square magnets inserted to demonstrate fit and side view. **c** Enlarged view of a well with a tube secured inside of a well on top of a magnet, showing that the magnet sits just below the bottom of the well plate and the tube is secured in the center of the well, from both a top and side view. **d** Demonstration of loading the inside and outside of the tube with a 10 µL pipette tip, example demonstrates 3 µL of seeding volume inside the tube and approximately 40 µL of seeding volume outside. **e** Fluorescent image taken 3 h after seeding and removal of center tube. H460 lung cancer island (red) and HDF-α fibroblasts (green) with distinct space of separation between the two cultures.

mice, and the cells can be fixed and stained after such longer-term studies to confirm the extent of growth and survivability of both the healthy and cancer cells. The online supplementary Figure 1 (for all online suppl. material, see https://doi.org/10.1159/000533773) shows zoomed-in images of the boundary over time. From these closer images, it can be observed that the H460 cancer cells contain both round tumor-like cells and elongated mesenchymal-like cells within the mass.

Fibroblast and Cancer Cell Interaction

Enhanced growth for cancer in the presence of fibroblasts found in other studies can be confirmed in this study. Seen in Figure 3, HDF-α increased the growth rate of the H460 cancer cells as the average island tumor mass in the co-culture device grew larger by 7% and 18% than the cancer cells grown by themselves, after normalizing for initial seeding differences. The increased growth and evident metastasis zones seen in Figure 2 Day 7 indicate that the co-culture mimics the effects seen by numerous other researchers, particularly the boosted growth and increased metastasis phenotype-like cancer cells. Under standard conditions, H460 cancer cells prefer to maintain cell-to-cell contact during their growth with very few cells moving away from the initial cancer mass which slows down the spread. However, H460 cancer cells robustly outgrew over the surrounding fibroblasts in the co-culture wells (Fig. 2b).

Co-Culture Drug Study

A panel of drugs was selected from common anti-cancer agents to drugs that may see some use in combination therapies and included a single dose in the IC(50) range for paclitaxel (Taxol), doxorubicin (Dox),

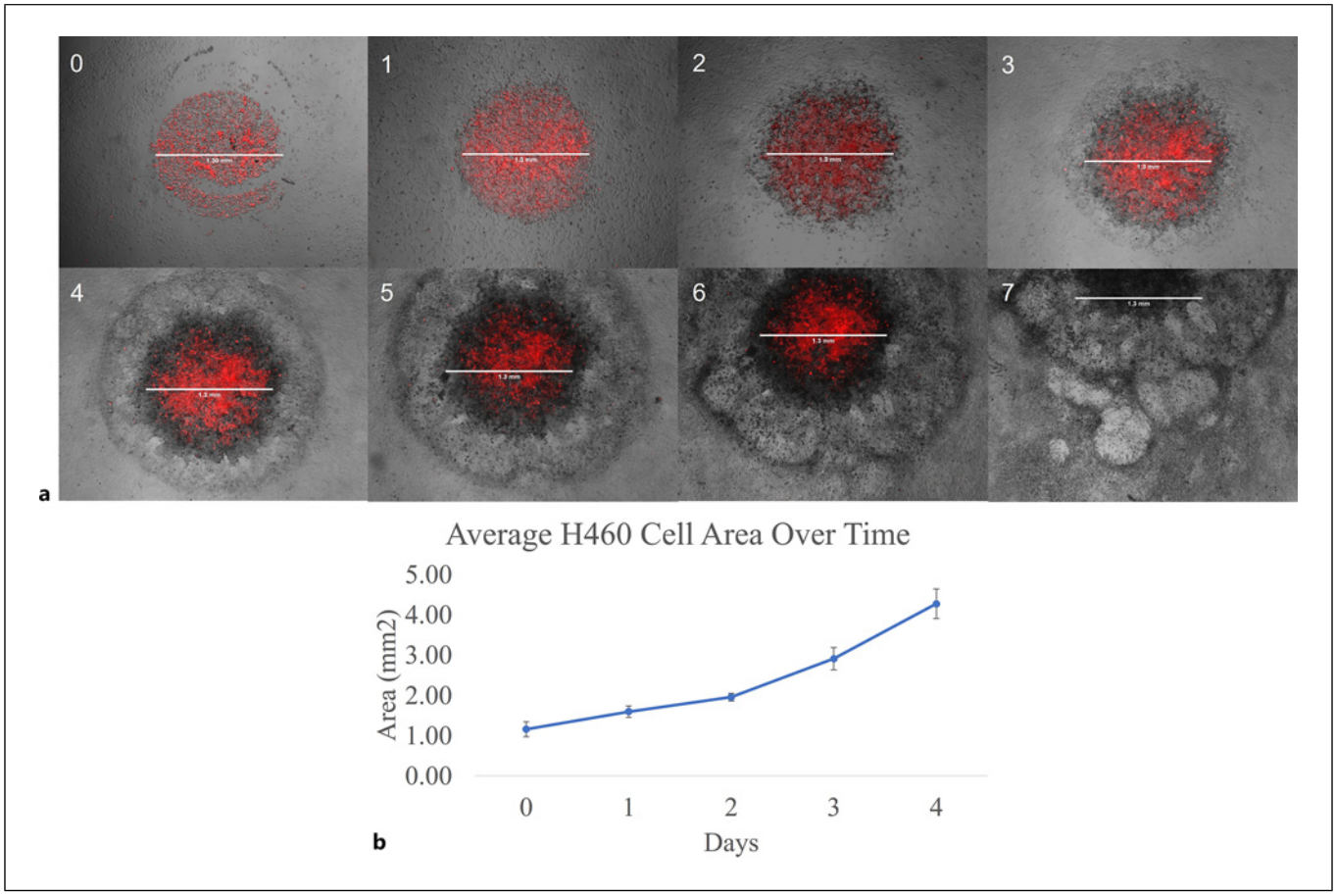

Fig. 2. Progression of H460 lung cancer cells surrounded by HDF-α fibroblast cells over 7 days. **a** Picture 0 taken 3 h after seeding, other pictures taken daily starting 24 h after picture 0 and ending on day 7. Red area is cell tracking dye CMTMR given to H460 cancer cells prior to seeding and enhanced in ImageJ after fluorescent microscopy. **b** Average cell area measured in ImageJ from the left to the right edges of the main cancer mass over the first 4 days, scale bars are 1.3 mm, and the inner diameter of the metal tube used for separation during seeding.

5-fluorouracil (5-FU), and chlorotoxin (CTX). The viability chart in Figure 4b below show the H460 viability results of the 48-hr drug study. Dox showed the greatest amount of cell death, but both populations of H460 and HDF-α cells can be seen to be suffering in the bright field image of Figure 4a. 5-FU reduced cancer cell viability by 75%, but healthy HDF-α cells can be seen in the brightfield image with intact nuclei, indicating that, while not as prolific as control, 5-FU may not be as universally toxic. Both Taxol and CTX mildly reduced cancer cell viability (not significantly), but clearly changed the boundary as a thinner fibroblast layer surrounding the central "tumor" mass can be seen in the respective brightfield images. The speed of the boundary formation between the H460 and HDF-α cells demonstrates that the drug screening can be used for rapid determination of efficacy and quantified with differential staining protocols and cell counting procedures.

Discussion

The cancer associated fibroblasts (CAFs) assist cancer cells in increasing their resistance and ability to metastasize from their main tumor area [10, 12, 29]. The current 3D co-culture devices for studying the mechanisms of the CAF action are important for guiding research informing therapeutic decisions involving more realistic CAF-cancer environments but lack simple method for testing different therapies in a quick and simple manner [19, 23, 26]. The present study takes advantage of a simple magnetic and 3D printable device that is adaptable to any common well-plate that facilitates rapid in vitro testing of therapeutics with a co-culture of CAF and cancer cells in a distinct island-type culture for straightforward visualization of results.

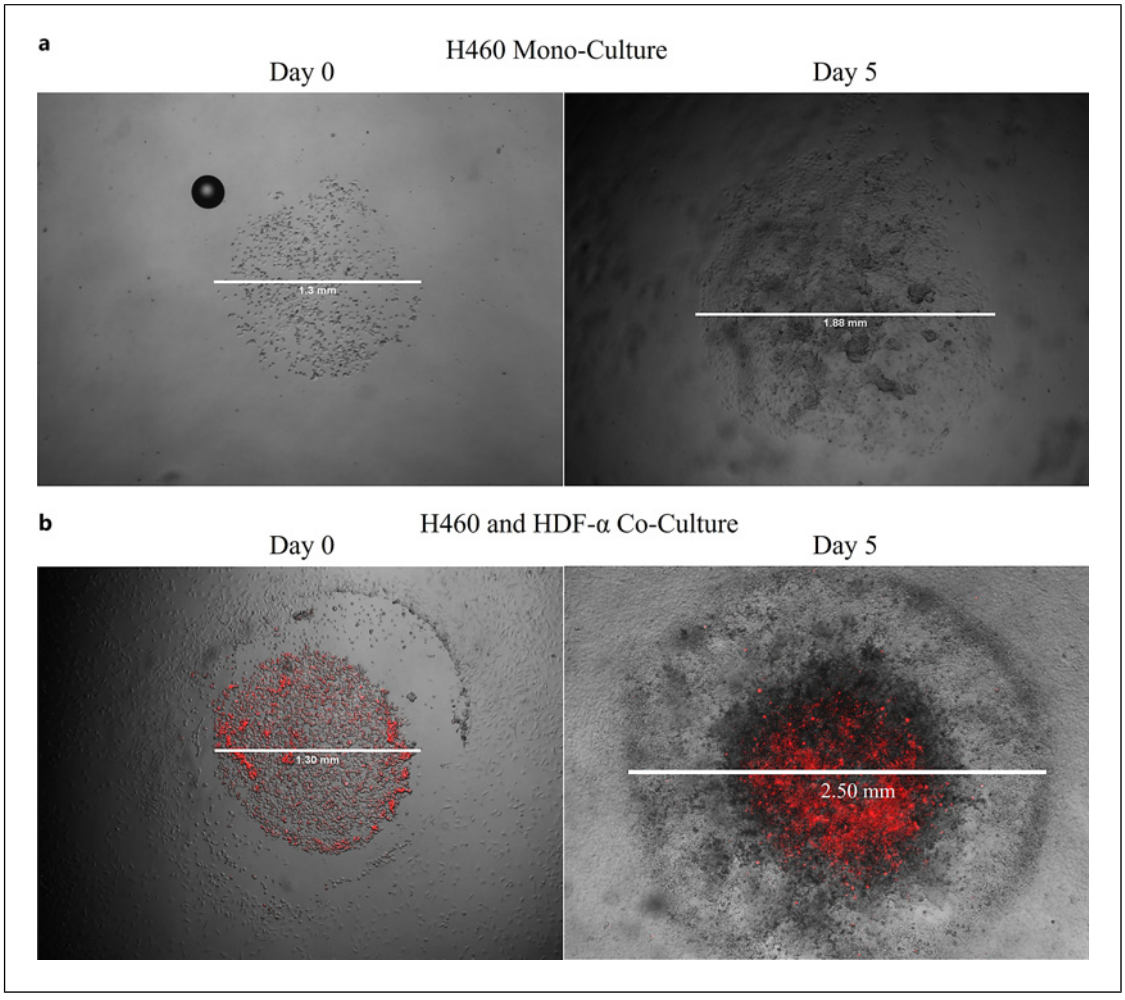

Fig. 3. Comparison of 5 days of growth for monoculture H460 lung cancer with co-culture H460 lung cancer and HDF-α. **a** Monoculture not stained and seeded at a density of 3,000 cells per well. **b** Co-culture H460 stained with CMTMR cell tracker prior to seeding and seeded at 5,000 cells per well and HDF-α not stained and seeded at 20,000 cells per well. Doubling time and expected area ratio normalized between the two seeding conditions. Brightfield images and fluorescent images adjusted in ImageJ.

Several studies have shown increased growth in cancer cells in the presence of fibroblasts [6, 8, 14], including a co-culture study that delved into relationships of organ-specific fibroblasts cultured with different organ cancer cells that showed some fibroblasts are more effective than others at improving cancer cell growth [14]. The present study utilized fibroblasts and lung cancer and the co-culture lung cancer cells expanded significantly faster than monoculture lung cancer cells and formed noticeable boundary layers when contacting the fibroblasts. This accelerated co-culture tumor growth model can form these CAF-cancer relationships and allow drug studies to be completed within 72 h of seeding time so that a large amount of information can be gathered quickly about drug-cancer-fibroblast interactions. Additionally, longer length recovery studies can be run to determine if recovery of cancer and fibroblast cells occurs post-treatment.

A challenge of device is that the fibroblasts do not produce a full extra-cellular matrix (ECM) environment [30, 31], and thus the full complement of metastatic cell movement and ECM degradation methods cannot be studied effectively with the current set up of the experiment. This leads the co-culture device to be stronger at determining toxicity or limiting drug studies to targeting the mechanical movement properties of cancer cells. There are some methods of inducing ECM production from fibroblasts [32, 33], but these methods will increase both the complexity of

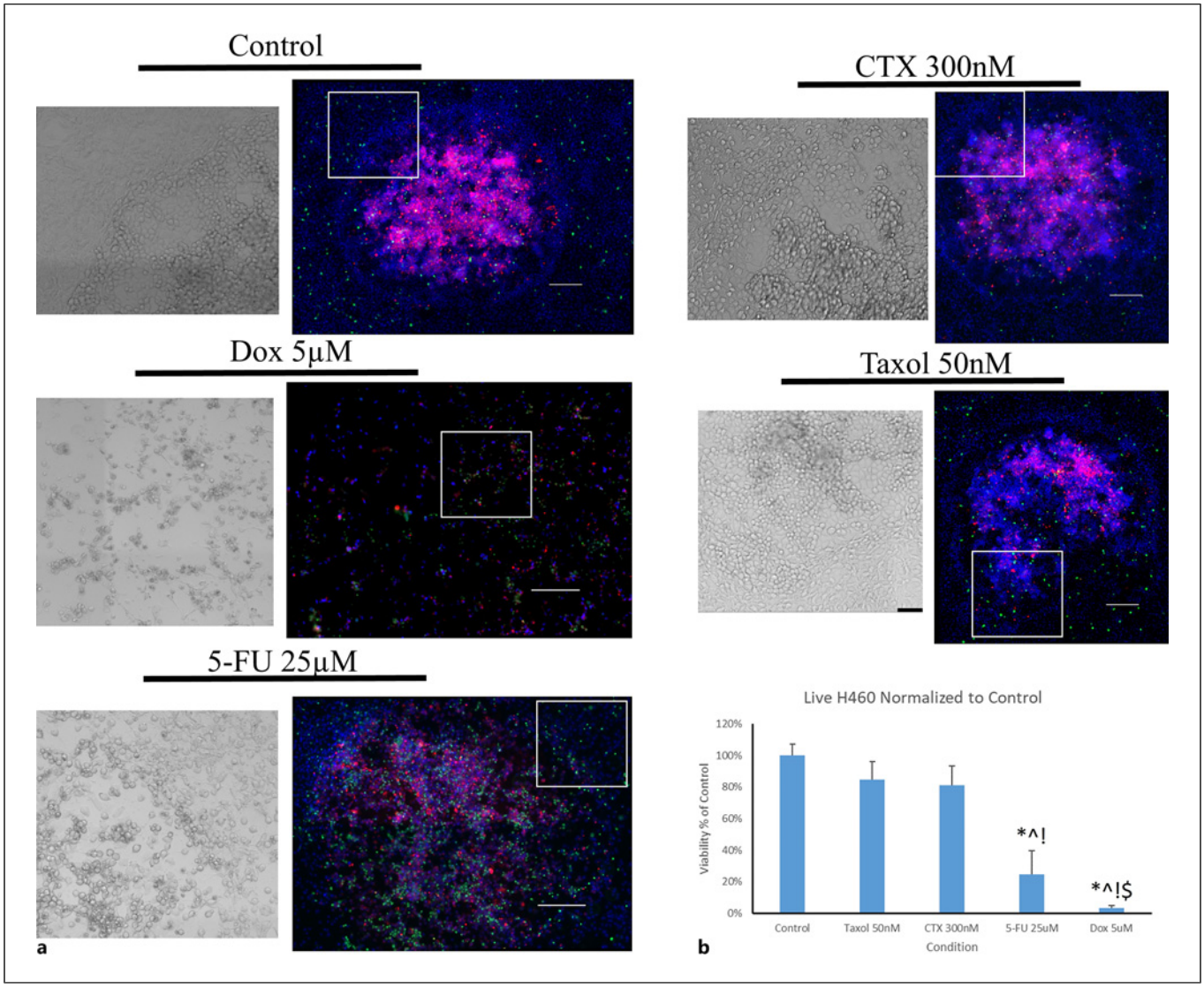

Fig. 4. H460 and HDF-α viability and boundary condition affected by various drug dosages. **a** Fluorescent images include H460 cells stained with CMTMR cell tracking dye prior to seeding for fluorescent imaging and after 48 h of incubation with drugs and no media changes, cells were stained with Hoechst and green live/dead stain for 20 min. Scale bar in all fluorescent images is 200 μm. Brightfield image is a zoom in of the same image at the location indicated by the white square to observe cell viability condition and morphology. Brightfield and fluorescent images were merged and adjusted in ImageJ for clarity. **b** Cell counting of live cancer cells was accomplished by utilizing ImageJ particle analyzer to count the Hoechst + CMTMR stained cells and subtracting the green live/dead stained cells and then normalized to control values to convert to percentage viability. *indicates statistical difference from control at $\alpha = 0.05$. ^indicates statistical difference from Taxol 50 nM at $\alpha = 0.05$. !indicates statistical difference from CTX 300 nM at $\alpha = 0.05$. $indicates statistical difference from 5-FU 25 μM at $\alpha = 0.05$.

the experiment and the time required to perform each iteration and so would need to be evaluated separately for if they could improve the mimicking of in vivo conditions.

Interestingly, several studies have determined that CAFs should be a therapeutic target to help fight against cancer growth [4, 8, 14]. Targeting the environment of cancer cells in conjunction with the cancer itself is a potentially effective method of dealing with cancer but may have some side effects if normal cell functions such as those demonstrated in paracrine signaling studies [15, 16] are targeted to help suppress the cancer. Our target for therapeutics is to either allow the healthy cells to thrive or at least leave enough alive to regrow after treatments are completed and the cancer cells are eliminated. The drug

study demonstrated that the Taxol dose had less toxicity for the HDF-α while also killing some of the H460 cells compared to the Dox and 5-FU conditions that killed all cells in the well indiscriminately. Comparing the drugs, Taxol appears to be more the attractive target to improve upon than Dox or 5-FU since the former can potentially allow regrowth of healthy cells when the treatment ends, while CTX would need synergistic drugs to take advantage of its effects on cancer cells.

In conclusion, the results demonstrated that the co-culture device can be seeded with healthy fibroblasts and cancer cells and create an accelerated growth model with the capability of studying large amounts of therapeutics on multiple cell types simultaneously.

Acknowledgments

We thank Dr. Qionghua Shen and Dr. Joseph Wolf for kindly providing training in imaging and analysis.

Statement of Ethics

An ethics statement is not required since there were no animal or human studies involved.

Conflict of Interest Statement

All authors reviewed the manuscript and declared no competing financial interests.

Funding Sources

This work was supported by the Institutional Research Training Grant from the National Institute of Health (5T32HL134613).

Author Contributions

Y.T.K. was the principal investigator and conceived the idea. A.A.G. wrote the paper, designed the device, and provided the data. Y.T.K. and A.A.G. developed the idea, designed the experiments, and carried out all experiments.

Data Availability Statement

All data generated or analyzed during this study are included in this article. Further enquiries can be directed to the corresponding author, Y.T.K., upon reasonable request.

References

1 American Cancer Society. Cancer facts and figures. Atlanta: American Cancer Society; 2022.
2 Canadian Cancer Statistics Advisory Committee. Canadian Cancer Statistics: a 2020 special report on lung cancer. Toronto, ON: Canadian Cancer Society; 2020.
3 Sung H, Ferlay J, Siegel RL, Laversanne M, Soerjomataram I, Jemal A, et al. Global cancer statistics 2020: GLOBOCAN estimates of incidence and mortality worldwide for 36 cancers in 185 countries. CA Cancer J Clin. 2021;71(3):209–49.
4 Saforo D, Omer L, Smolenkov A, Barve A, Casson L, Boyd N, et al. Primary lung cancer samples cultured under microenvironment-mimetic conditions enrich for mesenchymal stem-like cells that promote metastasis. Sci Rep. 2019;9(1):4177–16.
5 Raskov H, Orhan A, Gaggar S, Gögenur I. Cancer-associated fibroblasts and tumor-associated macrophages in cancer and cancer immunotherapy. Front Oncol. 2021;11:668731.
6 Koukourakis MI, Kalamida D, Mitrakas AG, Liousia M, Pouliliou S, Sivridis E, et al. Metabolic cooperation between co-cultured lung cancer cells and lung fibroblasts. Lab Invest. 2017;97(11):1321–31.
7 Liu XQ, Kiefl R, Roskopf C, Tian F, Huber RM. Interactions among lung cancer cells, fibroblasts, and macrophages in 3D co-cultures and the impact on MMP-1 and VEGF expression. PLoS One. 2016;11(5):e0156268.
8 Domen A, Quatannens D, Zanivan S, Deben C, Van Audenaerde J, Smits E, et al. Cancer-associated fibroblasts as a common orchestrator of therapy resistance in lung and pancreatic cancer. Cancers. 2021;13(5):987–22.
9 Prieto-García E, Díaz-García CV, Agudo-López A, Pardo-Marqués V, García-Consuegra I, Asensio-Peña S, et al. Tumor – stromal interactions in a co-culture model of human pancreatic adenocarcinoma cells and fibroblasts and their connection with tumor spread. Biomedicines. 2021;9(4):364.
10 Li S, Ou Y, Liu S, Yin J, Zhuo W, Huang M, et al. The fibroblast TIAM2 promotes lung cancer cell invasion and metastasis. J Cancer. 2019;10(8):1879–89.
11 Phan TKT, Shahbazzadeh F, Pham TTH, Kihara T. Alpha-mangostin inhibits the migration and invasion of A549 lung cancer cells. PeerJ. 2018;6(6):e5027.
12 Amann A, Zwierzina M, Gamerith G, Bitsche M, Huber JM, Vogel GF, et al. Development of an innovative 3D cell culture system to study tumour: stroma interactions in non-small cell lung cancer cells. PLoS One. 2014;9(3):e92511.
13 Fiorini E, Veghini L, Corbo V. Modeling cell communication in cancer with organoids: making the complex simple. Front Cell Dev Biol. 2020;8:166.
14 Koh B, Jeon H, Kim D, Kang D, Kim KR. Effect of fibroblast co-culture on the proliferation, viability and drug response of colon cancer cells. Oncol Lett. 2019;17(2):2409–17.
15 Ji X, Ji J, Shan F, Zhang Y, Chen Y, Lu X. Cancer-associated fibroblasts from NSCLC promote the radioresistance in lung cancer cell lines. Int J Clin Exp Med. 2015;8(5):7002–8.
16 Wang L, Cao L, Wang H, Liu B, Zhang Q, Meng Z, et al. Cancer-associated fibroblasts enhance metastatic potential of lung cancer cells through IL-6/STAT3 signaling pathway. Oncotarget. 2017;8(44):76116–28.
17 Majety M, Pradel LP, Gies M, Ries CH. Fibroblasts influence survival and therapeutic response in a 3D co-culture model. PLoS One. 2015;10(6):e0127948.

18 Movia D, Bazou D, Prina-Mello A. ALI multilayered co-cultures mimic biochemical mechanisms of the cancer cell-fibroblast cross-talk involved in NSCLC MultiDrug resistance. BMC Cancer. 2019;19(1):854–21.
19 Mi S, Du Z, Xu Y, Wu Z, Qian X, Zhang M, et al. Microfluidic co-culture system for cancer migratory analysis and anti-metastatic drugs screening. Sci Rep. 2016;6:35544.
20 Yu T, Guo Z, Fan H, Song J, Liu Y, Gao Z, et al. Cancer-associated fibroblasts promote non-small cell lung cancer cell invasion by upregulation of glucose-regulated protein 78 (GRP78) expression in an integrated bionic microfluidic device. Oncotarget. 2016;7(18): 25593–603.
21 Fong E, Tzlil S, Tirrell DA. Boundary crossing in epithelial wound healing. Proc Natl Acad Sci USA. 2010;107(45):19302–7.
22 Jain A, Bharadwaj P, Heeg S, Parzefall M, Taniguchi T, Watanabe K, et al. Minimizing residues and strain in 2D materials transferred from PDMS. Nanotechnology. 2018; 29(26):265203.
23 Horie M, Saito A, Noguchi S, Yamaguchi Y, Ohshima M, Morishita Y, et al. Differential knockdown of TGF- β ligands in a interaction model of lung cancer. BMC Cancer. 2014; 14:580.
24 Lewis KJR, Hall JK, Kiyotake EA, Christensen T, Balasubramaniam V, Anseth KS. Epithelial-mesenchymal crosstalk influences cellular behavior in a 3D alveolus-fibroblast model system. Biomaterials. 2018;155: 124–34.
25 Oh YS, Choi MH, Shin JI, Maza PAMA, Kwak JY. Co-culturing of endothelial and cancer cells in a nanofibrous scaffold-based two-layer system. Int J Mol Sci. 2020;21(11): 4128–3.
26 Bresciani G, Hofland LJ, Dogan F, Giamas G, Gagliano T, Zatelli MC. Evaluation of spheroid 3D culture methods to study a pancreatic neuroendocrine neoplasm cell line. Front Endocrinol. 2019;10:682–10.
27 Yaman S, Anil-Inevi M, Ozcivici E, Tekin HC. Magnetic force-based microfluidic techniques for cellular and tissue bioengineering. Front Bioeng Biotechnol. 2018;6:192.
28 Magnetic 3D bioprinting: high-throughput spheroid imaging and analysis using perkinelmer ensighttm multimode plate reader. 2020. Available from: http://classtap.pbworks.com/f/SkillSoft+-+Blended+Elearning.pdf.
29 Asif PJ, Longobardi C, Hahne M, Medema JP. The role of cancer-associated fibroblasts in cancer invasion and metastasis. Cancers. 2021;13(8):4720.
30 Smithmyer ME, Sawicki LA, Kloxin AM. Hydrogel scaffolds as in vitro models to study fibroblast activation in wound healing and disease. Biomater Sci. 2014;2(5):634–50.
31 Marinkovic M, Sridharan R, Santarella F, Smith A, Garlick JA, Kearney CJ. Optimization of extracellular matrix production from human induced pluripotent stem cell-derived fibroblasts for scaffold fabrication for application in wound healing. J Biomed Mater Res. 2021;109(10):1803–11.
32 Juhl P, Bondesen S, Hawkins CL, Karsdal MA, Bay-Jensen AC, Davies MJ, et al. Dermal fibroblasts have different extracellular matrix profiles induced by TGF-β, PDGF and IL-6 in a model for skin fibrosis. Sci Rep. 2020;10(1): 17300.
33 van Haasterecht L, Dsouza C, Ma Y, Korkmaz HI, de Jong Y, Ket JCF, et al. In vitro responses of human dermal fibroblasts to mechanical strain: a systematic review and meta-analysis. Front Mech Eng. 2023;9.